Proceedings of
ASME TURBO EXPO 2001
June 4-7, 2001, New Orleans, Louisiana

2001-GT-0311

A TEST CASE FOR THE NUMERICAL INVESTIGATION OF WAKE PASSING EFFECTS ON A HIGHLY LOADED LP TURBINE CASCADE BLADE

Peter Stadtmüller, Leonhard Fottner

Institut für Strahlantriebe
Universität der Bundeswehr München
D-85577 Neubiberg
Germany
Peter.Stadtmueller@unibw-muenchen.de

ABSTRACT

The paper presents a compilation of experimental data on the effects of wake-induced transition on a highly loaded LP turbine cascade intended to be used for further numerical work. Although the underlying physics is not yet completely understood, the benefits of wake passing are already known and employed in the design process of modern gas turbines. For further optimizations, the next step seems to be now to enable numerical simulations detailed enough to capture the major effects while being as uncomplicated as possible at the same time to be cost-effective. The experimental results constituted in this systematic investigation are available for download and should serve as a basic data set for future calculations with different turbulence and transition models, thereby shedding some light on the complexity and modeling required for a suitable numerical treatment of the wake-induced transition process.

The data introduced in this test case was acquired using a turbine cascade called T106D-EIZ with increased blade pitch compared to design point conditions in order to achieve a higher loading. A large separation bubble forms on the suction side and allows to study boundary layer development in great detail. The upstream blade row was simulated by a moving bar type wake generator. The measurements comprise hot wire data of the bar wake characteristics in the cascade inlet plane (velocity deficit and turbulence level), boundary layer surveys with surface-mounted hot films sensors and a hot wire probe at various locations and measurements of the total pressure loss coefficient. Unsteady pressure transducers are embedded into the suction side of a cascade blade and in a wake rake to resolve the local pressure distributions over time. They yield quantitative values easily comparable to the output of numerical simulations.

The objective of this paper is to enable and to invite interested researchers to validate their code on the data set. From the extensive test program, a very limited number of operating points have been selected to focus the work. The standardized data files include a "reference" case with an exit Reynolds number of 200.000 and an exit Mach number of 0.4 as well as two points with higher Mach or lower Reynolds number for constant wake passing frequencies and background turbulence levels.

NOMENCLATURE

Latin

c_{ax}	[m/s]	axial velocity
c_p	[-]	pressure coefficient
d	[m]	diameter
e	[m]	distance of the measurement plane
E	[V]	Voltage
f	[Hz]	frequency
l	[m]	chord length
p	[hPa]	pressure
T	[s]	bar passing period
t	[m], [s]	pitch, time
u	[m]	coordinate in circumferential direction
U	[m/s]	bar velocity

x	[m]	blade surface position
w	[m/s]	relative velocity

Greek

ω	[-]	total pressure loss
β	[°]	flow angle
Δ	[-]	difference between two values

Abbreviations

CTA	Constant Temperature Anemometry
DNS	Direct Numerical Simulation
EIZ	Generator of unsteady inlet flow condititions
M	Midspan
Ma	Mach number
PS	pressure side
Sr	Strouhal number $Sr = f*l/c_{ax}$
SS	suction side
Re	Reynolds number
TE	trailing edge

Subscripts

0	conditions for flow speed zero
1	cascade inlet plane
2	cascade exit plane
2th	downstream conditions for isentropic flow
ax	axial
b	bar
K	tank conditions
RMS	Root Mean Square
t	total
x	local

INTRODUCTION

Due to the existence of upstream blade rows, the flow in LP turbines is inherently unsteady. For the low Reynolds number conditions typically prevailing in LP turbines, the transition from laminar to turbulent flow is the main source of loss generation and significantly affected by the unsteady flow behavior. While there exists already considerable knowledge on laminar and turbulent flow conditions, the transitional region remains one of the main challenges for researchers. The many interacting parameters that influence boundary layer development and have to be considered for the design process of LP turbine blades imply that an optimization of the blade configuration can be achieved at reasonable cost on a numerical basis only. The high resolution results of the computations can then in return be used to improve the understanding of the experimental data.

First experimental investigations on the influence of wake passing on boundary layer development started as early as 1982 when Pfeil et al. (1983) used wakes generated by steel bars to investigate how this affects laminar to turbulent transition on a cylinder. Hodson (1983) studied the impact of wakes on the loss generation process in a LP turbine and proved together with Addison (1989) that wake passing can suppress a laminar separation bubble. A classification of different transition mechanisms was attempted by Mayle (1991), who identified the free stream turbulence, the pressure gradient and the strength of the wake as major parameters associated with the effects of wake passing. Schobeiri et al. (1995) reported that an increase in the wake passing frequency (or Strouhal number) has the same effect as a higher free stream turbulence level. The maybe best-known and most comprehensive tests were performed by Halstead et al. (1995) on a large scale research compressor and a LP turbine to reveal the fundamental effects of wake passing like early onset of transition whenever a wake travels across the blade surface, the suppression of a laminar separation bubble and the existence of the becalmed region. Curtis et al. (1996) showed that by considering unsteady flow conditions in the design process, the blade loading can be increased without sacrificing performance. A model presented by Schulte and Hodson (1997) can be used for the modeling of the becalmed region. Multistage investigations with surface-mounted hot films on a five stage LP turbine are reported e.g. by Arndt (1991).

High blade passing frequencies require costly and complex fast-response measurement systems. Therefore, the presently available data comprises mostly of time-averaged values. This agrees with commonly used design tools that are constricted to a quasi-steady treatment of the real turbomachinery flow instead of the time-consuming numerical modeling of the unsteady flow behavior. The next goal is an adequate numerical handling of the unsteady flow by developing a model that is able to predict the aerodynamic performance of the blade by considering the effects of wake passing. This calls for a profound understanding of the dynamic process and displays a need not only for time-averaged, but also for fluctuating flow quantities. To be able to gain confidence and to validate the results produced by numerical simulations, comprehensive unsteady data is required.

Unsteady codes are already used for modeling unsteady boundary layer development. Regarding the determination of the location and length of the transitional region, they often rely on empirical correlations and run the risk that experimental data is generalized and not universally applicable. Another possible way is to use a turbulence model which requires less experimental input, but is equally uncertain due to the limited abilities of the modeling of turbulence. As commonly used low Reynolds number k-ε models require a large spatial resolution, newer approaches apply a one-equation model in the near-wall region together with empirical correlations for the transition onset and the length of the transitional region. Fan and Lakshminarayana (1994) presented calculations with an unsteady inviscid solver coupled with a boundary layer code which includes an advanced k-ε model. A modified version of the one-equation model formulated by Spalart and Allmaras (1992) together with Drela's formulation of the Abu-Ghannam/Shaw transition criteria (1980) is implemented in the time-accurate Navier-Stokes solver TRACE_U. Using this code, results presented by Eulitz (1999) are compared to measurements on the original T106A cascade (without increased pitch) and show that this kind of modeling is capable of reproducing the effects of wake passing on the transition process. An example of a multistage LP turbine calculation – again with the TRACE_U code – can be found in Höhn and Heinig (2000). First incompressible DNS calculations on the T106A cascade have been performed at Stanford by Wu and Durbin (2000).

The test case presented in this paper provides time-averaged as well as time-resolved data regarding the boundary layer development on the suction side of a LP turbine blade and the loss generation process. Surface mounted hot film sensors are used to measure the qualitative distribution of unsteadiness and the quasi wall shear stress. Fast-

response miniature pressure transducers are embedded into the suction side blade surface and in a wake rake to measure quantitative pressure values. Static pressure tappings on the blade surface are used to measure the blade loading and to double-check the readings of the unsteady pressure probes. The bar wake characteristics are documented with 1D hot wire measurements. 3D hot wire traverses in the cascade inlet plane and boundary layer traverses in the rear part of the suction side are planned until this test case becomes available to complete the data basis. Numerical work using the data basis presented in this paper is already in progress using the TRACE_U code developed by DLR Cologne and will be discussed in a separate paper.

The work presented is part of a joint research effort on unsteady flows in turbomachines. As the validation process should move gradually from simplified to more complex conditions, the program includes measurements on a flat plate (TU Berlin), in a turbine cascade (this paper) and in a low speed compressor rig (TU Dresden) as well as numerical work at DLR Cologne (RANS) and TU Karlsruhe (DNS and heat transfer). An overview of the complete project is given by Hourmouziadis (2000).

EXPERIMENTAL APPARATUS

Turbine Cascade

The measurements were performed on a large scale LPT cascade consisting of five aft-loaded blades which represent the mid-span section of the PW2037 LPT rotor blade. As the objective was to increase the lift coefficient by about 30%, blade pitch was raised to t/l=1.05 as compared with design point conditions (t/l=0.799) in order to achieve a higher blade loading. The blade geometry was not adapted accordingly and a large separation bubble forms on the suction side starting at approximately 60% axial chord. The coordinates of the T106 profile in the bitangential and axial coordinate system are included in the test case. The aerodynamic data at design point conditions as well as the definition of angles and distances can be extracted from Fig. 1.

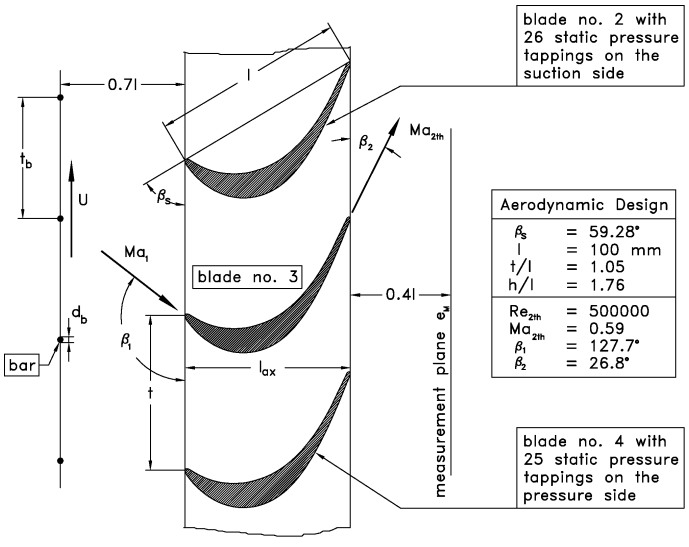

Fig. 1: T106D-EIZ cascade design

Test Facilities

All experimental data presented in this test case was obtained at the High-Speed Cascade Wind Tunnel of the Universität der Bundeswehr München (Fig. 2). This continuously operating open loop facility is situated inside a pressurized tank. It allows Mach and Reynolds numbers to be varied independently in order to achieve flow conditions typical for turbojet engines. The turbulence intensity in the test section can be adjusted using different turbulence grids upstream of the nozzle. The air is supplied by a six-stage axial compressor, driven by a 1.3 MW a.c. electric motor which is situated outside the pressure tank. The air enters through a diffuser into the settling chamber, where it is cooled down to an adjustable constant temperature between 30°C and 60°C. The flow then accelerates through a nozzle towards the wind tunnel throat with the blade cascade mounted at its exit. A more detailed description of the facility can be found e.g. in Sturm and Fottner (1985). The following data were used to monitor the flow conditions of the cascade main flow: the total temperature in the settling chamber, the static pressure in the tank (downstream conditions) and the static and total pressure of the main flow upstream of the cascade. The cascade always consists of an odd number of blades of which merely the center blade is being used for the measurements. The two adjacent blades were instrumented with additional static pressure tappings to evaluate the profile loading.

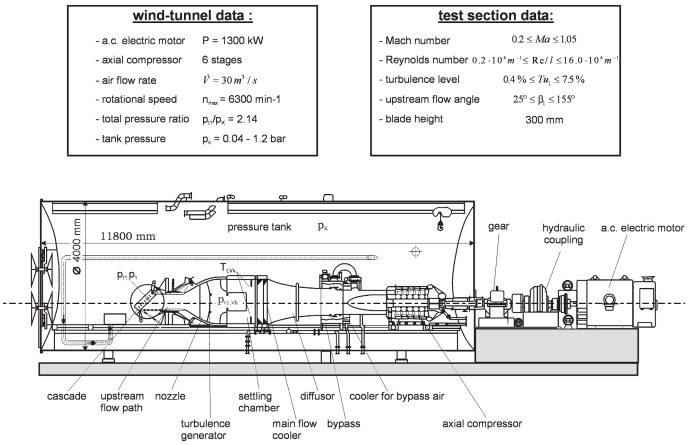

Fig. 2: High-Speed Cascade Wind Tunnel (HGK)

The periodically unsteady flow caused by the relative motion of rotor and stator rows and its influence on the turbine cascade is simulated by a moving bar type wake generator with a bar diameter ratio of d_b/l=0.02. The cylindrical steel bars create a far wake very similar to the one produced by an actual airfoil (Pfeil and Eifler, 1976). Preliminary tests showed that the wakes shed by bars of 2 mm diameter are representative for the wakes of the T106 profile geometry regarding the wake width. The velocity deficit and the turbulence level inside the bar wake are slightly higher if compared to the T106 blade wake. The distance ratio between the bars and the cascade inlet plane is about x/l = 0.7 (see Fig. 1). The belt mechanism drives the bars with speeds of up to 40 m/s, thus generating Strouhal numbers between 0.42 and 1.68 for the investigated test cases. This so-called EIZ (Erzeuger Instationärer Zuströmung, see Fig. 3) and its constructional principles are explained by Acton and Fottner (1996) in more detail. However, it

should be noted that the maximum bar speed of 40 m/s is still too slow to produce a Strouhal number and inlet velocity triangle representative for modern gas turbines. The data acquired with this setup is therefore not suited for the in-depth analysis of boundary layer development in real turbines.

Another difficulty is the loss of mass flow through the gaps at the upper and lower end of the cascade, which are required to be able to move the bars upstream of the cascade inlet plane. Although adjustable guide vanes were mounted at the upper and lower wind tunnel wall to achieve a constant inlet pressure distribution, this causes the inlet flow angle to diverge from the geometric flow angle that should results from the installation and to be inhomogeneous over the cascade height. There is no loss of mass flow through the side walls. Previous numerical work showed a change in the inlet flow angle of about +5° for the center blade by comparing different numerically computed blade loadings for various flow angles with the measured pressure distribution. Therefore the first step for all numerical work seems to be a matching of the profile pressure distribution for steady flow conditions with the corresponding experimental data (the bar upstream of the cascade were removed) by iteratively varying the inflow angle. The necessary files for the steady inflow are included in the data set. Planned 3D hot wire measurements in the cascade inlet plane will provide additional information on the flow angle and its variation in circumferential direction, but are not yet available.

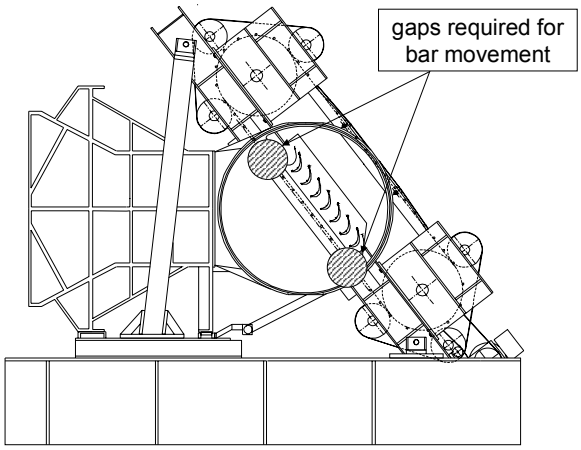

Fig. 3: Moving Bar Wake Generator (EIZ)

Oil-and-Dye visualizations and flow field traverses with a five hole probe at midspan were taken to ensure that the flow field was two-dimensional and unaffected by secondary flow effects.

EXPERIMENTAL DATA

Test Program

From the extensive test program as described in Stadtmüller et al. (2000), three operating points are extracted and presented in this test case. Point **1** should serve as a reference with Point **2** describing a variation of the exit Mach number and Point **3** showing the influence of a decrease in the exit Reynolds number with all other parameters remaining unchanged. An overview of the relevant parameters for the numerical simulation for each data point is compiled in Tab. 1.

A compact but complex summary of typical experimental results is shown in Fig. 4. Within the scope of this paper, they will be presented in principle, but only be discussed briefly. A more detailed description is available in Stadtmüller et al. (2000).

	Point 1	**Point 2**	**Point 3**
Exit Reynolds number Re_{2th}	200.000	200.000	60.000
Exit Mach number Ma_{2th}	0.4	0.59	0.4
Geometric inlet flow angle β_1 [°]	127.7	127.7	127.7
Total pressure in the inlet plane p_{t1} [hPa]	259.6	190.5	77.7
Static pressure in the inlet plane p_1 [hPa]	242.5	166.3	72.7
Total temperature T_{t1} [°C]	40.1	40.1	40.1
Bar spacing t_b [mm]	40	40	40
Bar speed U_b [m/s]	21.4	21.4	21.4
Strouhal number Sr	0.84	0.63	0.84
Background turbulence level Tu_1	< 1%	≈ 1 %	< 1%
Turbulence level in the bar wake	7 %	6 %	4 %
Bar wake amplitude	15 %	16 %	11 %
Total pressure loss coefficient ω	0.061	0.046	0.112

Tab. 1: Test program data

Cascade Inlet Conditions

The data for the total pressure p_{t1} and the static pressure p_1 is measured with a pitot probe and static wall taps located 500 mm upstream of the cascade inlet plane. As this is also upstream of the bars, they do not represent the correct values for the conditions in the cascade inlet plane. A correction that is described in the section dealing with the total pressure losses has been performed for the data set presented in this test case. A standard 1D hot wire probe was used to measure the turbulence intensity inside and outside the wake and the velocity deficit caused by the bars. Calibration was performed in-situ for each operating point before running the experiment using a 4^{th} order polynomial. The number of points was large enough to correctly reproduce the slope of the calibration curve for the calculation of the turbulence level. Fig. 4a shows that the background turbulence level for Point **1** is below 1% outside the wake and reaches a maximum value of 7% in the center of the bar wake. The velocity deficit as well as the wake width can be easily extracted from the figure. The available data will be completed with 3D hot wire measurements in the cascade inlet plane to gain information on the turbulent time and length scales in the near future.

Measurement of the Blade Loading

The loading of the cascade was measured by means of 26 static pressure tappings on the suction side and 25 static pressure tappings on the pressure side of the adjacent blades (see Fig. 1) connected to a Scanivalve system. The local static pressures p_x measured with the tappings on the profile surface are used to calculate the local pressure distribution coefficient $c_{p,x}$ and the isentropic Mach number $Ma_{is,x}$ (Eq. 1 and Eq. 2)

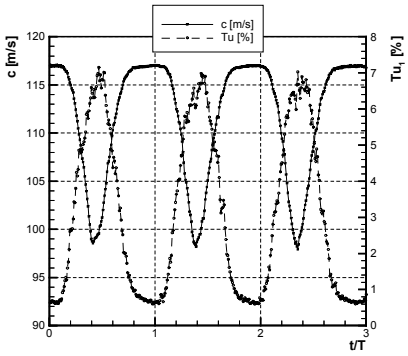

a) 1D-Hot wire measurements in the cascade inlet plane, Point **1**

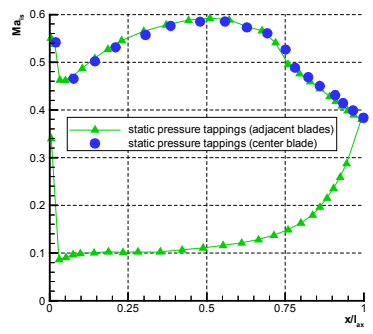

b) Isentropic Mach number distribution on the center and adjacent blades, time-averaged, Point **1**

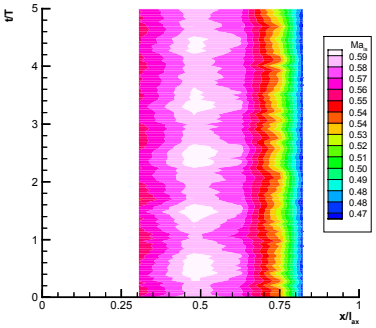

c) Isentropic Mach number distribution on the center blade, time-resolved, Point **1**

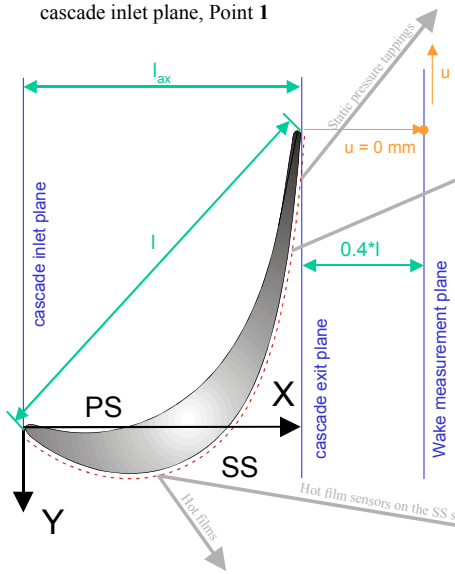

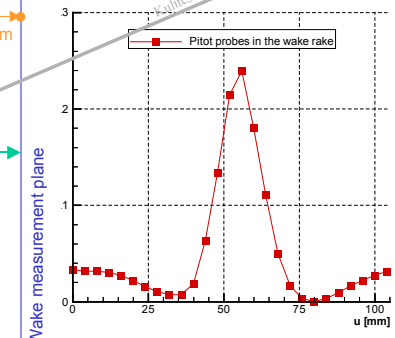

d) Total pressure losses in the wake measurement plane, time-averaged, Point **1**

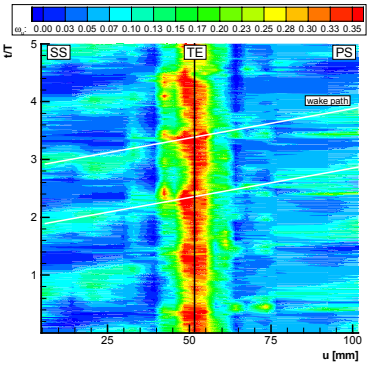

e) Total pressure losses in the wake measurement plane, time-resolved, $Ma_{2th} = 0.4$, $Re_{2th} = 200.000$, $t_b = 80$ mm, $U_b = 10.7$ m/s

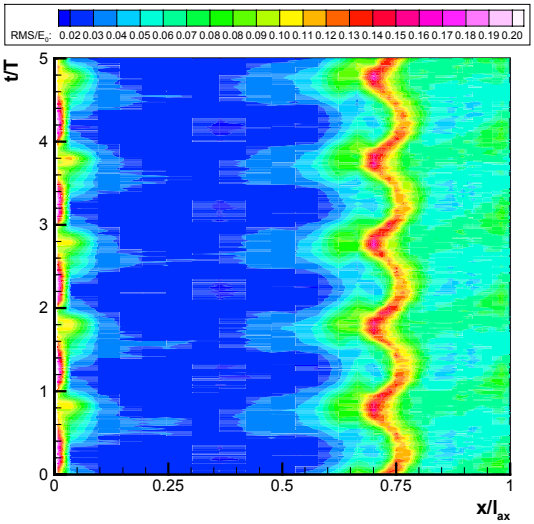

f) RMS values measured with surface-mounted hot films on the suction side, time-resolved, Point **1**

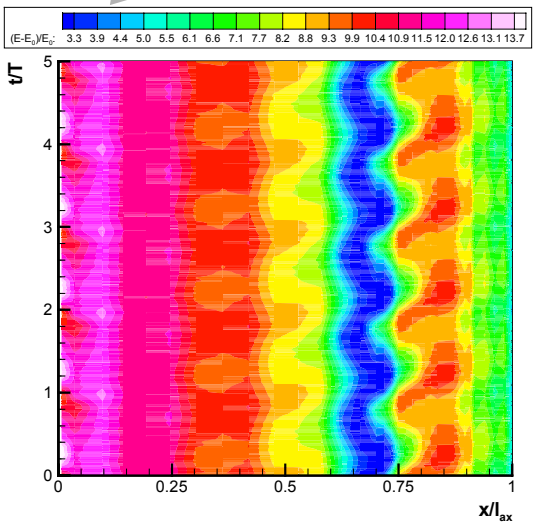

g) Quasi wall shear stress measured with surface-mounted hot films on the suction side, time-resolved, Point **1**

Fig. 4: Experimental results for the T106D-EIZ cascade

$$c_{p,x} = \frac{p_x - p_K}{p_{t1} - p_K} \qquad \text{(Eq. 1)}$$

$$Ma_{is,x} = \sqrt{\frac{2}{\kappa - 1} \cdot \left[\left(\frac{p_{t1}}{p_x} \right)^{\frac{\kappa-1}{\kappa}} - 1 \right]} \qquad \text{(Eq. 2)}$$

The isentropic Mach number distribution for Point **1** is plotted in Fig. 4b. The change in inlet flow angle compared to design conditions (which are no longer valid due to the increase in blade pitch) results in a suction peak close to the leading edge. Following the flow acceleration on the suction side, a separation bubble forms starting at about $0.65*x/l_{ax}$. The tappings on the center and adjacent blades yield almost identical data indicating that the change in the inlet flow angle in circumferential direction is very small for this operating point.

The time-resolved profile loading was determined from a total of six *Kulite* LQ-125 fast-response pressure sensors embedded into the suction side of the center blade. Additional static pressure tappings were placed at the same chord position as the *Kulite* sensors (see Fig. 4b). Five-hole probe traverses behind the original (plain) blade and the one with integrated sensors showed no measurable influence of the instrumentation regarding total pressure losses or outlet flow angle.

The *Kulite* sensors were connected to a 14 channel signal amplifier with integrated low-pass filter (eight-pole Butterworth; 48 dB/Octave) before being digitized with a 12-bit A/D-converter at a sampling rate of 62.5 kHz/channel. A once-per-revolution trigger mechanism ensured that the wake passing effects were studied for wakes produced by identical bars. Data processing for the unsteady case was done according to Eq. 1 and 2 using the well-established PLEAT technique (Phase Locked Ensemble Averaging Technique, Lakshminarayana et al., 1974) in order to separate random and periodic signals. A total of 500 ensembles was recorded for each run.

Ensemble-averaged results for five fast-response sensors on the suction side are shown in Fig. 4c where non-dimensionalized wake passing time along the ordinate is plotted over non-dimensionalized axial chord length along the abscissa. The velocity deficit in the wake lowers the maximum isentropic Mach number so that the five wake passing events are clearly visible around $0.5*x/l_{ax}$. The limited spatial resolution with a total of only six working sensors will be improved by adding four additional transducers in the laminar and transitional region. In the test case the data files include the time-resolved static wall pressures measured with the calibrated Kulite sensors as well as the sensor location on the suction side surface. Of course the pressure do not provide any information on the boundary layer state or the location of the transitional region, but are intended as another mean to compare experimental and numerical work.

Measurement of Total Pressure Loss

The averaged and time-resolved aerodynamic performance of the center blade at different operating points was evaluated by computing stagnation pressure losses with a new fast-response wake rake (see Fig. 5) downstream of the cascade exit plane.

The design of the new wake rake is similar to that of a pitot rake and has been validated in previous measurements with a traversing five-hole probe. The fast response sensors are paired with conventional pitot probes which are able to provide the mean pressure values (with the limitations as described in Weyer 1975) while the semiconductor chips are used to measure the fluctuating component. The sensors are used in differential pressure mode with the reference pressure p_{t1} being supplied through the probe shaft; this is similar to the probe design e.g. of Kupferschmied et al. (1998). As all transducers are oriented in the same plane, it is impossible to measure any flow angles. Errors resulting from blockage or dynamic flow effects around the probe head do not significantly affect the signals if compared to the data of the time-averaged measurements and results from five-hole probe traverses.

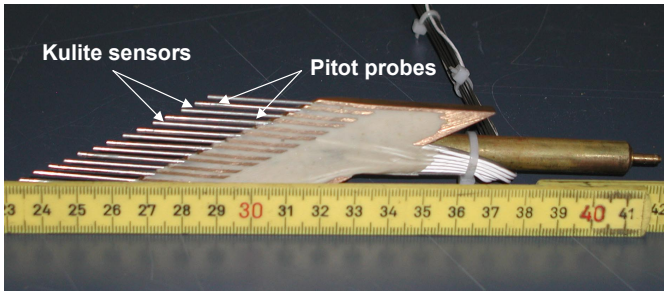

Fig. 5: Wake rake with *Kulite* sensors and conventional pitot probes

The data was evaluated using the conservative laws for mass, momentum and energy according to a procedure described by Amecke (1967) for the total pressure loss coefficient (Eq. 3)

$$\omega_u = \frac{p_{t1} - p_{t2,u}}{p_{t1} - p_K} \qquad \text{(Eq. 3)}$$

with $p_{t2,u}$ being measured with the sensors in the wake rake (steady for the pitot probes and time-resolved for the *Kulites*) for every circumferential position of the transducers. As the pressure p_{t1} is measured upstream of the bars, the total pressure loss produced by the bars is assigned to the loss of the profile, which has to be corrected for later comparisons. For that reason, it is assumed that outside the wake the flow is isentropic, i.e. that no total pressure loss occurs in the cascade duct. The recorded loss outside the wake when traversing the wake rake must be caused by the bars, and this value is then deducted from the profile loss.

The set of data stored for each traverse position contains the coordinate of the sensor and the local total pressure loss coefficient computed according to Eq. 3. For the pitot probes, an example of the results is shown in Fig. 4d for Point **1**. The measured values have been integrated in circumferential direction to obtain the blade profile loss coefficient which is stated in Tab. 1. For the fast-response measurements, the data is plotted similar to the time-resolved isentropic Mach number distribution in the form of a space-time diagram (see Fig. 4e), but in this case for a much lower Strouhal number as the values for Point **1** are not analyzed yet. The wake moving from the suction side towards the blade surface, the interaction between boundary layer and wake and the wake path on the suction side are clearly detectable.

Surface-Mounted Hot Film Measurements

Arrays of surface-mounted hot film sensors were glued onto the suction side of the center blade to analyze the development of the boundary layer characteristics along the profile over time. The entire length of the suction surface was covered with a total of 36 gauges with their spacing varying between 2.5 and 5 mm. They consisted of a 0.4 µm thin nickel film applied by vapour deposition process onto a polyamide substrate and were logged simultaneously in sets of 12 sensors at sampling frequencies ranging from 40 to 60 kHz. The frequency response of the sensors was sufficient to resolve the first two harmonics of the bar passing frequency. As shown e.g. by Schröder (1991), the qualitative behavior of the boundary layer characteristics can be determined directly from the anemometer output and do not necessarily require an extensive calibration procedure. The anemometer data was low-pass filtered and digitized with a 12-bit A/D-converter before being stored on hard disks.

A total of 300 ensembles were logged with each run and evaluated for quasi-wall shear stress (Eq. 4) and random unsteadiness RMS (Eq. 5), where b represents the anemometer output voltage for the hot film results. To be able to compare the hot film sensors, the resulting values were normalized with the anemometer voltage at zero flow, thereby eliminating the influence of manufacturing differences between the gauges.

$$\tilde{b}(t) = \frac{1}{n} \cdot \sum_{j=1}^{n} b_j(t) \approx \frac{E(t) - E_0}{E} \qquad \text{(Eq. 4)}$$

$$\sqrt{\tilde{b}^2(t)} = \sqrt{\frac{1}{n-1} \cdot \sum_{j=1}^{n} (b_j(t) - \tilde{b}(t))^2} \approx \frac{E_{RMS}(t)}{E_0} \qquad \text{(Eq. 5)}$$

Typical results of the hot film measurements are shown as space-time diagrams in Fig. 4f and Fig. 4g. The first figure contains the RMS values computed according to Eq. 5 with the wake being identifiable at the leading edge from the high levels of turbulence. The wake path is again visible when elevated RMS values occur in the laminar region around $0.4*x/l_{ax}$ before triggering early transition at $0.7*x/l_{ax}$. The minimum values of quasi wall shear stress are of special interest in the second figure as they identify the location and extent of the separation bubble. It can be seen that every wake passing reduces the size of the bubble and that contrary to the measurements of Lou and Hourmouziadis (2000) the location where the bubble starts varies over time. It has to be kept in mind that the hot films are not calibrated, which allows only a phenomenological interpretation of the data.

Measurement Errors

The accuracy of the fast-response probes on the blade surface and in the wake rake is estimated to be ± 1 hPa (0.15% FS non-linearity and hysteresis according to the sensor specification plus additional errors from the amplification and digitalization process as well as electrical noise). The pressure tappings on the blade surface were measured with a Scanivalve system with an overall accuracy of ± 0.2 hPa. The reference pressures p_{t1} and p_K were read using a DPT6400 pressure scanner with an error of ± 0.2 hPa. The flow temperature T_t is accurate within ± 0.1 °C and changes no more than ± 0.05 °C during one measurement run. The positioning accuracy of the traversing system for the wake probe and the planned boundary layer traverses is within 0.01 mm.

As the hot films are not calibrated, their numerical values are not meaningful. This is also the reason why the values of quasi-wall shear stress do not reach values around zero in the separation bubble. However, it should be noted that the various measurement techniques are applied not simultaneously but sequentially, which results in slightly different test conditions (e.g. p_{t1} changes from 259.6 to 259.4 hPa) due to the limited repeatability capacities of the wind tunnel controlling system.

Numerical Work

Numerical calculations using the TRACE_U code are presently conducted and will provide an insight into the wake-boundary layer interaction process. First results for an operating point different to the ones included in this test case are presented in a separate paper. The location where the wake hits the suction side and the angle under which it enters the cascade inlet plane are especially interesting for the future analysis of the unsteady pressure data on the suction side. The limited accuracy of the fast-response sensors makes a detailed interpretation of the results difficult. A comparison of the measured time-resolved pressures with the output of numerical simulations might be extremely valuable to be able to assess the performance of the *Kulite* sensors.

CONCLUSIONS

A comprehensive experimental data set on the influence of wake passing on the boundary layer development and loss behavior of an LP turbine blade is summarized and meant as a contribution to the code validation process. The results are stored in standardized data files and available for download. A hyperlink is place on the web site of the institute at

http://www.unibw-muenchen.de/campus/LRT12/welcome.html

A highly loaded LP turbine cascade called T106D-EIZ is used for the investigations. The upstream blade row is simulated with a moving bar type wake generator. The experimental data includes a detailed description of the flow conditions in the cascade inlet plane by means of hot wire measurements. Surface-mounted hot film RMS values and quasi wall shear stress distributions provide time-resolved information on the location and extent of the transitional region and the boundary layer development. Static pressure tappings on the suction and pressure side blade surface yield time-averaged information on the blade loading. Calibrated static pressure values are available through miniature pressure transducers embedded into the suction side surface and easily comparable to the output of numerical simulations. Total pressure losses are measured with a wake rake instrumented with pitot probes as well as fast-response pressure sensors to acquire time-averaged and time-resolved data. Boundary layer traverses in the turbulent part of the suction side boundary layer and 3D hot wire traverses in the cascade inlet plane will complete the data set in the near future.

ACKNOWLEDGMENTS

The work reported in this paper was performed within the project "Periodisch instationäre Strömungen in Turbomaschinen" funded by the Deutsche Forschungsgemeinschaft. The permission for publication is gratefully acknowledged.

REFERENCES

Abu-Ghannam, B.J., Shaw, R., 1980, "*Natural Transition of Boundary Layers – The Effects of Turbulence, Pressure Gradient, and Flow History*", J. Mechanical Engineering Science, Vol. 22, No. 5

Acton, P., Fottner, L., 1996, "*The Generation of Instationary Flow Conditions in the High-Speed Cascade Wind Tunnel",* 13th Symposium on Measuring Techniques in Transonic and Supersonic Flow in Cascades and Turbomachines

Amecke, J., 1967, "*Auswertung von Nachlaufmessungen an ebenen Schaufelgittern*", Bericht 67A 49, AVA Göttingen

Arndt, N., 1991, "*Blade Row Interaction in a Multistage Low-Pressure Turbine*", ASME Paper 91-GT-283

Curtis, E.M., Hodson, H.P., Banieghbal, M.R., Denton, J.D., Howell, R.J., and Harvey, N.W., 1996, "*Development of Blade Profiles for Low Pressure Turbine Applications",* ASME Paper 96-GT-358

Eulitz, F., 1999, "*A RANS Method for the Time-Accurate Simulation of Wake-Induced Boundary Layer Transition in Turbine Flows*", AIAA-99-7275

Fan, S., Lakshminarayana, B., 1994, "*Computation and Simulation of Wake-Generated Unsteady Pressure and Boundary Layers in Cascades*", ASME Paper 94-GT-140/141

Halstead, D.E., Wisler, D.C., Okiishi, T.H., Walker, G.J., Hodson, H.P., Shin, H.-W., 1995, "*Boundary Layer Development in Axial Compressors and Turbines: Part 1-4*", ASME Paper 95-GT-461/462/463/464

Höhn, W., Heinig, K., 2000, "*Numerical and Experimental Investigation of Unsteady Flow Interaction in a Low Pressure Multistage Turbine*", ASME Paper 2000-GT-437

Hodson, H.P., 1983, "*Boundary Layer and Loss Measurements on the Rotor on an Axial Flow Turbine*", ASME Paper 83-GT-4

Hodson, H.P., Addison, J.S., 1989, "*Wake-Boundary Layer Interaction in an Axial Flow Turbine Rotor at Off-Design Conditions*", J. of Turbomachinery, Vol. 111, No. 2

Hourmouziadis, J., 2000, "*Das DFG Verbundvorhaben Periodisch Instationäre Strömungen in Turbomaschinen*", DGLR Jahrestagung

Kupferschmied, P., Köppel, P., Roduner, C., Gyarmathy, G., "*On the Development and Application of the FRAP® (Fast-Response Aerodynamic Probe) System for Turbomachines – Part I: The Measurement System*", ASME Paper 99-GT-152

Lakshminarayana, B., Poncet, A., 1974, "*A Method of Measuring Three-Dimensional Rotating Wakes behind Turbomachines*", J. of Fluids Engineering, June, Vol. 96, No. 2, pp. 87-91

Lou, W., Hourmouziadis, J., 2000, "*Separation Bubbles under Steady and Periodic Unsteady Main Flow Conditions*", ASME Paper 2000-GT-270

Mayle, R.E., 1991, "The Role of Laminar-Turbulent Transition in Gas Turbine Engines", ASME Paper 91-GT-261

Pfeil, H., Eifler, J., 1976, "*Turbulenzverhältnisse hinter rotierenden Zylindergittern*", Forschung i. Ingenieurwesen, Vol. 42, pp. 27-32

Pfeil, H., Herbst, R., Schröder, T., 1983, "*Investigation of the Laminar-Turbulent Transition of Boundary Layers Disturbed by Wakes",* J. of Engineering for Power, Vol. 105, pp. 130-137

Schobeiri, M.T., Read, K., Lewalle, J., 1995, "*Effect of Unsteady Wake Passing Frequency on Boundary Layer Transition: Experimental Investigation and Wavelet Analysis*", ASME Paper 95-GT-437

Schröder, T., 1991, "*Investigation of the Blade Row Interaction and Boundary Layer Transition Phenomena in a Multistage Aero Engine Low Pressure Turbine by Measurements with Hot-Film Probes and Surface-Mounted Hot-Film Gauges*", VKI Lecture Series Boundary Layers in Turbomachines, 1991-6

Schulte, V., Hodson, H.P., 1997, *"Prediction of the Becalmed Region for LP Turbine Profile Design*", ASME Paper 97-GT-398

Spalart, P.R., Allmaras, S.R., 1992*, "A One-Equation Turbulence Model for Aerodynamic Flows*", AIAA-92-0439

Stadtmüller, P., Fottner, L., Fiala, A., 2000, "*Experimental and Numerical Investigation of Wake-Induced Transition on a Highly Loaded LP Turbine at Low Reynolds Numbers*", ASME Paper 2000-GT-269

Sturm, W., Fottner, L.,1985, "*The High-Speed Cascade Wind Tunnel of the German Armed Forces University Munich",* 8th Symposium on Measuring Techniques in Transonic and Supersonic Flow in Cascades and Turbomachines

Weyer, H., 1975, "*On the Measurement of the Fluctuating Total and Static Pressure in Turbomachines Including the Determination of the Correct Time-Weighted Pressures*", in: Modern Methods of Testing Rotating Components of Turbomachines (Instrumentation), AGARD-AG-207

Wu, X., Durbin, P.A., 2000, "*Evidence of Longitudinal Vortices Evolved from Distorted Wakes in a Turbine Passage*", Paper submitted for publication to J. Fluid Mech.